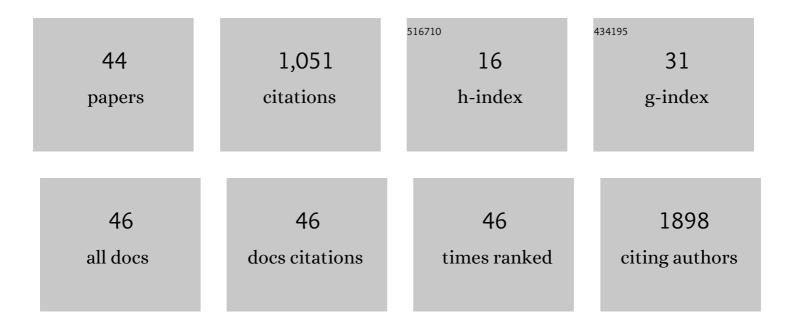
## Paul D Mcnaughter

List of Publications by Year in descending order

Source: https://exaly.com/author-pdf/6859957/publications.pdf Version: 2024-02-01



#	Article	IF	CITATIONS
1	Nanostructured Aptamer-Functionalized Black Phosphorus Sensing Platform for Label-Free Detection of Myoglobin, a Cardiovascular Disease Biomarker. ACS Applied Materials & Interfaces, 2016, 8, 22860-22868.	8.0	208
2	In Situ Synthesis of PbS Nanocrystals in Polymer Thin Films from Lead(II) Xanthate and Dithiocarbamate Complexes: Evidence for Size and Morphology Control. Chemistry of Materials, 2015, 27, 2127-2136.	6.7	84
3	Shining a light on transition metal chalcogenides for sustainable photovoltaics. Chemical Science, 2017, 8, 4177-4187.	7.4	84
4	Copperâ€Doped CdSe/ZnS Quantum Dots: Controllable Photoactivated Copper(I) Cation Storage and Release Vectors for Catalysis. Angewandte Chemie - International Edition, 2014, 53, 1598-1601.	13.8	58
5	The effect of alkyl chain length on the structure of lead( <scp>ii</scp> ) xanthates and their decomposition to PbS in melt reactions. Dalton Transactions, 2016, 45, 16345-16353.	3.3	45
6	Novel Xanthate Complexes for the Size-Controlled Synthesis of Copper Sulfide Nanorods. Inorganic Chemistry, 2017, 56, 9247-9254.	4.0	39
7	Nanoparticle–sulphur "inverse vulcanisation―polymer composites. Chemical Communications, 2015, 51, 10467-10470.	4.1	35
8	On the stability of surfactant-stabilised few-layer black phosphorus in aqueous media. RSC Advances, 2016, 6, 86955-86958.	3.6	35
9	3-Aryl-3-(trifluoromethyl)diazirines as Versatile Photoactivated "Linker―Molecules for the Improved Covalent Modification of Graphitic and Carbon Nanotube Surfaces. Chemistry of Materials, 2011, 23, 3740-3751.	6.7	32
10	Black phosphorus with near-superhydrophobic properties and long-term stability in aqueous media. Chemical Communications, 2018, 54, 3831-3834.	4.1	28
11	Facile synthesis of a PbS <sub>1â^'x</sub> Se <sub>x</sub> (0 ≤i>x ≤) solid solution using bis( <i>N</i> , <i>N</i> -diethyl- <i>N</i> ′-naphthoylchalcogenoureato)lead( <scp>ii</scp> ) complexes. New Journal of Chemistry, 2018, 42, 16602-16607.	2.8	27
12	Nickel-Doped Ceria Nanoparticles: The Effect of Annealing on Room Temperature Ferromagnetism. Crystals, 2015, 5, 312-326.	2.2	26
13	The deposition of PbS and PbSe thin films from lead dichalcogenoimidophosphinates by AACVD. Inorganica Chimica Acta, 2016, 453, 439-442.	2.4	23
14	VUV photodissociation dynamics of diatomic gold, Au2: A velocity map imaging study at 157nm. Chemical Physics Letters, 2009, 483, 10-15.	2.6	21
15	Doping Group IIB Metal Ions into Quantum Dot Shells via the Oneâ€Pot Decomposition of Metalâ€Dithiocarbamates. Advanced Optical Materials, 2015, 3, 704-712.	7.3	19
16	A SPION-eicosane protective coating for water soluble capsules: Evidence for on-demand drug release triggered by magnetic hyperthermia. Scientific Reports, 2016, 6, 20271.	3.3	19
17	The influence of precursor on rhenium incorporation into Re-doped MoS <sub>2</sub> (Mo <sub>1â^xx</sub> Re <sub>x</sub> S <sub>2</sub> ) thin films by aerosol-assisted chemical vapour deposition (AACVD). Journal of Materials Chemistry C, 2017, 5, 9044-9052.	5.5	18
18	A Thin Silica–Polymer Shell for Functionalizing Colloidal Inorganic Nanoparticles. Angewandte Chemie - International Edition, 2011, 50, 10384-10387.	13.8	16

PAUL D MCNAUGHTER

#	Article	IF	CITATIONS
19	SWCNT photocathodes sensitised with InP/ZnS core–shell nanocrystals. Journal of Materials Chemistry C, 2016, 4, 3379-3384.	5.5	15
20	On-demand, magnetic hyperthermia-triggered drug delivery: optimisation for the GI tract. Journal of Materials Chemistry B, 2016, 4, 1704-1711.	5.8	15
21	PbS x Se1â^'x thin films from the thermal decomposition of lead(II) dodecylxanthate and bis(N,N-diethyl-N′-naphthoylselenoureato)lead(II) precursors. Journal of Materials Science, 2018, 53, 4283-4293.	3.7	15
22	High magnetic relaxivity in a fluorescent CdSe/CdS/ZnS quantum dot functionalized with MRI contrast molecules. Chemical Communications, 2017, 53, 10500-10503.	4.1	14
23	Synthesis of (Bi <sub>1â^'x</sub> Sb <sub>x</sub> ) <sub>2</sub> S <sub>3</sub> solid solutions <i>via</i> thermal decomposition of bismuth and antimony piperidinedithiocarbamates. RSC Advances, 2019, 9, 15836-15844.	3.6	14
24	Synthesis and characterization of carbon nanotubes covalently functionalized with amphiphilic polymer coated superparamagnetic nanocrystals. Journal of Colloid and Interface Science, 2012, 383, 110-117.	9.4	13
25	The <i>in situ</i> synthesis of PbS nanocrystals from lead(II) <i>n</i> -octylxanthate within a 1,3-diisopropenylbenzene–bisphenol A dimethacrylate sulfur copolymer. Royal Society Open Science, 2017, 4, 170383.	2.4	13
26	A low cost synthesis method for functionalised iron oxide nanoparticles for magnetic hyperthermia from readily available materials. Faraday Discussions, 2014, 175, 83-95.	3.2	12
27	Bi-phasic titanium dioxide nanoparticles doped with nitrogen and neodymium for enhanced photocatalysis. Nanoscale, 2015, 7, 17735-17744.	5.6	11
28	Important Phase Control of Indium Sulfide Nanomaterials by Choice of Indium(III) Xanthate Precursor and Thermolysis Temperature. European Journal of Inorganic Chemistry, 2019, 2019, 1421-1432.	2.0	11
29	Enabling electrochemical studies of chemically-modified carbon nanotubes in non-aqueous electrolytes using superparamagnetic nanoparticle-nanotube composites co-modified by diazirine molecular "tethers†Electrochemistry Communications, 2011, 13, 1139-1142.	4.7	9
30	Plasmonically enhanced electromotive force of narrow bandgap PbS QD-based photovoltaics. Physical Chemistry Chemical Physics, 2018, 20, 14818-14827.	2.8	9
31	Full compositional control of PbS <sub>x</sub> Se <sub>1â^x</sub> thin films by the use of acylchalcogourato lead( <scp>ii</scp> ) complexes as precursors for AACVD. Dalton Transactions, 2018, 47, 16938-16943.	3.3	8
32	Accessing γ-Ga <sub>2</sub> S <sub>3</sub> by solventless thermolysis of gallium xanthates: a low-temperature limit for crystalline products. Dalton Transactions, 2019, 48, 15605-15612.	3.3	8
33	Tunable structural and optical properties of CuInS2 colloidal quantum dots as photovoltaic absorbers. RSC Advances, 2021, 11, 21351-21358.	3.6	8
34	Heterometallic 3d–4f Complexes as Air-Stable Molecular Precursors in Low Temperature Syntheses of Stoichiometric Rare-Earth Orthoferrite Powders. Inorganic Chemistry, 2020, 59, 15796-15806.	4.0	7
35	Copper-complexed isonicotinic acid functionalized aluminum oxide nanoparticles. Main Group Chemistry, 2015, 15, 1-15.	0.8	6
36	Controlled aggregation of quantum dot dispersions by added amine bilinkers and effects on hybrid polymer film properties. RSC Advances, 2015, 5, 95512-95522.	3.6	6

#	Article	IF	CITATIONS
37	Investigating the Effect of Steric Hindrance within CdS Single-Source Precursors on the Material Properties of AACVD and Spin-Coat-Deposited CdS Thin Films. Inorganic Chemistry, 2022, 61, 8206-8216.	4.0	6
38	In Vivo Applications of Inorganic Nanoparticles. , 2011, , 185-220.		5
39	Photoelectrochemical Formation of Polysulfide at PbS QD-Sensitized Plasmonic Electrodes. Journal of Physical Chemistry Letters, 2019, 10, 5357-5363.	4.6	5
40	Tunable structural, morphological and optical properties of undoped, Mn, Ni and Ag-doped CuInS2 thin films prepared by AACVD. Materials Science in Semiconductor Processing, 2022, 137, 106224.	4.0	5
41	Precursor determined lateral size control of monolayer MoS <sub>2</sub> nanosheets from a series of alkylammonium thiomolybdates: a reversal of trend between growth media. Chemical Communications, 2017, 53, 6428-6431.	4.1	4
42	Synthesis of molybdenum-doped rhenium disulfide alloy using aerosol-assisted chemical vapour deposition. Materials Science in Semiconductor Processing, 2021, 127, 105718.	4.0	4
43	Structural Investigations of α-MnS Nanocrystals and Thin Films Synthesized from Manganese(II) Xanthates by Hot Injection, Solvent-Less Thermolysis, and Doctor Blade Routes. ACS Omega, 2021, 6, 27716-27725.	3.5	3
44	Ricinoleic Acid as a Green Alternative to Oleic Acid in the Synthesis of Doped Nanocrystals. ChemistrySelect, 2018, 3, 13548-13552.	1.5	2